Probabilistic calibration of a Greenland Ice Sheet model using spatially-resolved synthetic observations: toward projections of ice mass loss with uncertainties

Won Chang (1)*, Patrick J. Applegate (2), Murali Haran (1), Klaus Keller (3)

5

(1) Department of Statistics, Pennsylvania State University, University Park, PA 16802

(2) Earth and Environmental Systems Institute, Pennsylvania State University, University Park, PA 16802

(3) Department of Geosciences, Pennsylvania State University, University Park, PA 16802

10   * Corresponding author.   E-mail address: wuc130@psu.edu

Abstract

15   Computer models of ice sheet behavior are important tools for projecting future sea level rise. The simulated modern ice sheets generated by these models differ markedly as input parameters are varied. To ensure accurate ice sheet mass loss projections, these parameters must be constrained using observational data. Which model parameter combinations make sense, given observations? Our method assigns probabilities to parameter combinations based on how well the model reproduces the

20   Greenland Ice Sheet profile. We improve on the previous state of the art by accounting for spatial information, and by carefully sampling the full range of realistic parameter combinations, using statistically rigorous methods. Specifically, we estimate the joint posterior probability density function of model parameters using Gaussian process-based emulation and calibration. This method is an important step toward probabilistic projections of ice sheet contributions to sea level rise, in that it uses

25   observational data to learn about parameter values. This information can, in turn, be used to make

projections while taking into account various sources of uncertainty, including parametric uncertainty, data-model discrepancy, and spatial correlation in the error structure. We demonstrate the utility of our method using a perfect model experiment, which shows that many different parameter combinations can generate similar modern ice sheet profiles. This result suggests that the large

30   divergence of projections from different ice sheet models is partly due to parametric uncertainty. Moreover, our method enables insight into ice sheet processes represented by parameter interactions in the model.

35   **1. Introduction**

Accurate projections of future sea level rise are important for present-day adaptation decisions. Global mean sea level has risen 0.2-0.3 m over the last two to three centuries (e.g. Church and White 2006; Jevrejeva et al. 2008), and this rise is expected to continue in the future (Meehl et al. 2007). A

40   significant fraction of world population and built infrastructure lies near present-day sea level, and these people and resources are at risk from sea level rise. Projections of sea level rise with sound characterization of the associated uncertainties can inform the design of risk management strategies (e.g., Lempert et al., 2012).

45   Here, we focus on the Greenland Ice Sheet component of future sea level rise, as estimated by ice sheet models. Computer models of ice sheet behavior make up an important member of a suite of methods for projecting sea level rise. Enhanced mass loss from the Greenland Ice Sheet is just one component of overall sea level rise, which also includes contributions from the Antarctic Ice Sheets, small glaciers, thermal expansion of ocean water, and the transfer of water stored on land to the oceans. However, the

50   Greenland Ice Sheet is a large potential contributor to sea level rise, and also a highly uncertain one; if

this ice sheet were to melt completely, sea level would rise by about 7 m (Bamber et al. 2001, 2013; Lemke et al. 2007), and both the rate of ice loss and its final magnitude are uncertain (Lenton et al. 2008). Present estimates of future sea level rise are derived primarily from semi-empirical extrapolations of tide gauge data (e.g., Rahmstorf 2007; Grinsted et al. 2009; Jevrejeva et al. 2012) and

55 expert assessments of future ice sheet behavior (e.g., Pfeffer et al. 2008; Bamber and Aspinall 2013). Ice sheet models complement these methods, in that they provide internally-consistent representations of the processes that are important to the growth and decay of ice sheets. Although imperfect, such models have been the focus of intense development effort since the fourth Intergovernmental Panel on Climate Change assessment report (e.g., Bindschadler et al. 2013).

60

To yield accurate projections, ice sheet models must be started from an initial condition that resembles the real ice sheet as closely as possible, both in terms of the spatial distribution of ice and the temperature distribution within the ice body. Ice flow is driven primarily by thickness and surface slope (e.g., Alley et al. 2010), and warm ice deforms more easily than cold ice. Similarly, the melt rate

65 of a patch of the ice sheet's surface is strongly sensitive to its elevation (Born and Nisancioglu 2012). Thus, errors in the initial condition used for ice sheet model projections will lead to inaccuracies in simulated future ice distributions and sea level rise contributions. In practice, all models include simplifications that also affect projection accuracy (e.g., Kirchner et al. 2011), perhaps more than initial condition errors. However, matching the modern ice sheet is a frequently-recurring theme in the

70 literature (e.g., Ritz et al. 1997; Greve, 1997; Huybrechts 2002; Stone et al. 2010; Greve et al. 2011; Pollard and DeConto 2012).

The initial condition used in ice sheet models is a function of input parameter values, as well as the spinup method. Because the thermal field within the ice sheet is incompletely known, most modeling

75 studies perform an initialization to bring the simulated ice sheet to a state that is consistent with the

present-day climatology (e.g., Stone et al. 2010), climate model output (e.g., Fyke et al. 2011), or climate history estimated from ice cores (e.g., Applegate et al. 2012). Most models allow the simulated ice sheet's surface topography to evolve during the spinup period; thus, the estimated initial condition usually does not exactly match the observed ice sheet topography (Bamber et al. 2001, 2013).

80   For example, many studies obtain a simulated modern Greenland ice sheet that is larger than expected (e.g. Heimbach et al. 2008; Stone et al. 2010; Robinson et al. 2010; Vizcaino et al. 2010; Greve et al. 2011; cf. Bamber et al. 2001, 2013). Ice sheet models have many uncertain parameters that affect the softness of the ice, the speed of basal sliding, and the intensity of surface melting, among other processes (Ritz et al. 1997; Hebeler et al. 2008; Stone et al. 2010; Fitzgerald et al. 2011; Applegate et al.

85   2012). Adjusting these parameters changes the simulated modern ice sheet (Stone et al. 2010; Applegate et al. 2012).

Despite the importance of achieving a good match between ice sheet model output and the present-day ice geometry, it remains unclear how to use data on the modern ice sheet to assess the relative

90   plausibility of different model runs. The root-mean-squared error (RMSE) is sometimes used for this purpose (e.g., Greve and Otsu 2007; Stone et al., 2010). However, it is unclear how to translate the RMSE values from a set of model runs into probabilistic projections of ice volume change, as required for sea level studies. Using a probability model that accounts for various uncertainties, as we do here, helps overcome this limitation.

95

Recent work by McNeall et al. (2013) partly addresses this challenge by using highly-aggregated metrics describing the Greenland ice sheet's geometry (volume, area, and maximum thickness; Ritz et al. 1997; Stone et al. 2010). Specifically, McNeall et al. (2013) train a statistical emulator (e.g., Sacks et al. 1989; Kennedy and O'Hagan 2001) to relate input parameter combinations to model output, using

100   a previously-published ensemble of ice sheet model runs (Stone et al. 2010). The work of McNeall et

al. (2013) is groundbreaking in its application of a computationally-efficient statistical emulator to an ice sheet model, allowing estimation of model output at many more design points than would have been possible with the model itself. However, the highly-aggregated metrics used by McNeall et al. (2013) neglect information on the spatial distribution of ice, which might further limit the parameter combinations that agree well with the observed geometry of the modern ice sheet.

A second challenge involves characterizing the effects of input parameter choice on the agreement between modeled and observed ice sheets. In an ensemble of Greenland Ice Sheet model runs carried out by Applegate et al. (2012; described below), the parameter combinations that agree well with the modern ice sheet's volume are widely distributed over parameter space, with no easily-discernable structure. This result may arise from uncharacterized interactions among the model parameters. This outcome also has strong implications for model projections of sea level rise from the ice sheet, in that the model runs that agree well with the modern volume constraint give widely diverging sea level rise projections (Applegate et al. 2012).

Finally, estimates of future sea level rise require projections of ice volume change with well-characterized uncertainties. Perturbed-parameter ensembles (e.g., Stone et al. 2010; Applegate et al. 2012) represent an important step toward this goal, but the relatively small number of model runs that can be performed in a reasonable time (usually 10^2-10^3; Stone et al. 2010; Applegate et al. 2012) are insufficient to fully explore model parameter space. As McNeall et al. (2013) demonstrate, statistical emulators help overcome this dimensionality problem; however, the objective function mentioned above is also needed to assign plausibility scores to the emulator output.

Here, we address these challenges using a Bayesian framework that combines data, models, and prior beliefs about model input parameter values. Like McNeall et al. (2013), we train an emulator on an

5

ensemble of ice sheet model runs. However, we build on their work by using an explicit likelihood function, and by incorporating information from a north-south profile of average ice thicknesses. Specifically, we use a Gaussian process emulator to estimate the first 10 principal components of the zonal mean ice thickness profile, following a recent climate model calibration study (Chang et al. 2013; this procedure explains more than 90% of the variance in mean ice thickness values). Further, we perform a perfect model experiment to investigate the interactions between input parameters. Our approach recovers the correct parameter values and projected ice volume changes from an "assumed-true" model realization, and the multi-dimensional probability density function displays expected physical interactions (Section 1.2.1, below). These interactions were not evident from the simple analysis employed by Applegate et al. (2012, their Fig. 1).

The paper proceeds as follows. In the remainder of the Introduction, we describe the ensemble that we use to train the emulator. In Section 2, we outline our method for using a Gaussian process emulator to estimate the principal components of the zonally-averaged ice thicknesses, and the setup of our perfect model experiment. Section 3 presents the results of the perfect model experiment. In Section 4, we conclude by pointing out the implications of our work, as well as its limitations and potential directions for future research.

1.2. The ensemble

We train our emulator with a 100-member perturbed-parameter ensemble described in Applegate et al. (2012). This ensemble uses the three-dimensional ice sheet model SICOPOLIS (Greve, 1997; Greve et al. 2011). Each model run spans the period from 125,000 years ago (125 ka BP) to 3500, driven by surface temperature and sea level histories derived from geologic data (Imbrie et al. 1984; Dansgaard et al. 1993; Johnsen et al. 1997). SICOPOLIS is a shallow ice-approximation model, meaning that it

neglects longitudinal stresses within the ice body (Kirchner et al. 2011). Like most ice sheet models, it also includes many simplifications in calculating the surface mass balance, notably through its use of the positive degree-day method for relating surface temperatures to melting (Braithwaite, 1995; Calov and Greve 2005; van der Berg et al. 2011). These simplifications improve SICOPOLIS' computational

155 efficiency relative to higher-order or full-Stokes models (e.g., Seddik et al. 2012), allowing it to be run repeatedly over 10^5-yr time scales.

The parameter combinations in the Applegate et al. (2012) ensemble were chosen by Latin hypercube sampling (McKay et al. 1979), following the earlier work of Stone et al. (2010). Latin hypercube

160 sampling distributes points throughout parameter space more efficiently than Monte Carlo methods (Urban and Fricker 2010). In their experiment, Applegate et al. (2012) varied the ice flow enhancement factor, the ice and snow positive degree-day factors, the geothermal heat flux, and the basal sliding factor (cf. Ritz et al. 1997; Stone et al. 2010; Fitzgerald et al. 2011). These parameters control the softness of ice, the rapidity with which the ice sheet's surface lowers at a given temperature,

165 the amount of heat that enters the base of the ice sheet, and the speed of sliding at a given stress (see Applegate et al. 2012 for an explanation of how each parameter affects model behavior).

McNeall et al. (2013) trained their emulator using a perturbed-parameter ensemble of ice sheet model runs published by Stone et al. (2010). Key differences between the Applegate et al. (2012) ensemble

170 and the Stone et al. (2010) ensemble involve the processes included in the simulations and the parameters varied in the ensembles. The model used by Stone et al. (2010; Glimmer v. 1.0.4; see Rutt et al. 2009) neglects basal sliding, a process included in the SICOPOLIS runs presented by Applegate et al. (2012). Consequently, Stone et al. (2010) varied the lapse rate instead of the basal sliding factor adjusted by Applegate et al. (2012).

175

The results presented by Applegate et al. (2012) suggest that widely diverging ice sheet model parameter values yield comparable modern ice sheets, but substantially different sea level rise projections. Applegate et al. (2012) assessed the plausibility of their model runs by comparing the simulated ice volumes in 2005 to the estimated modern ice volume (Bamber et al. 2001; Lemke et al. 2007); those runs that yielded modern ice volumes within 10% of the estimated value were kept. These plausible runs yielded a range of future sea level rise projections that was ~75% of the median estimate.

Moreover, the parameter combinations that agree well with the modern ice volume constraint are widely distributed over parameter space. With the exception of the ice positive degree-day factor, where only values less than ~15 mm day^{-1} $^{O}C^{-1}$ satisfy the ice volume constraint, no pattern emerges from the distribution of the successful runs through parameter space. McNeall et al. (2013) make a similar point using their own results. Statistically, this inability to learn about the plausibility of various parameter combinations given observations is termed an "identifiability problem."

1.2.1. Expected interactions among model input parameters

The apparently-structureless distribution of successful runs through parameter space (Applegate et al. 2012, their Fig. 1) may stem from interactions among the parameters. The parameters can be loosely grouped into those that control the ice sheet's surface mass balance (the ice and snow positive degree-day factors) and those that control ice movement (the ice flow enhancement factor, the basal sliding factor, and the geothermal heat flux). Either group of parameters can cause mass loss from the ice sheet to be high or low, given fixed values of the parameters in the other group. For example, a high ice positive degree-day factor should be associated with a low snow positive degree-day factor to produce the same amount of melt as a model run with more moderate values of both parameters. This

interaction is bounded, however, because the maximum snow positive degree-day factor is much lower than the maximum value for ice; also, at the peak of the ablation season, there is no snow left on the lower parts of the ice sheet, so the ice positive degree-day factor dominates over part of the year. Similarly, the same ice velocities can be produced by either a high flow enhancement factor and a low basal sliding factor, or the reverse. Basal sliding can be a much faster process than ice flow, so this parameter interaction is also bounded. However, basal sliding operates only where the bed is thawed, and the geothermal heat flux likely controls the fraction of the bed that is above the pressure melting point.

The relatively small number of design points in the ensemble presented by Applegate et al. (2012) hinders mapping of the interactions among parameters over their five-dimensional space. Coherent mapping requires many more design points, but performing these additional runs with the full ice sheet model is impractical because of the model's high computational cost. This problem suggests a need for a computationally efficient emulator to fill the gaps in parameter space between the existing model runs.

2. Methods

As described above, our goals are 1) to identify a method for quantifying the agreement between ice sheet model output and observations that incorporates spatial information, 2) to characterize the interactions among input parameters, and 3) to produce illustrative projections of sea level rise from the Greenland Ice Sheet based on synthetic data. In this section, we provide an outline of our methods for achieving these goals; fuller descriptions appear in Chang et al. (2013) and in the Supplementary Information.

We accomplish goal #1 through identifying a statistical model that results in a "likelihood function." Together with assumed prior probabilities and ice thickness observations, this statistical model can be used to assign posterior probabilities to individual parameter combinations. The details of the statistical model, and the resulting likelihood function, are given in the Supplementary Information.

To achieve goal #2, we perform a "leave-one-out" perfect model experiment with a Gaussian process emulator, a computationally-cheap surrogate for the full ice sheet model. In this type of cross-validation, the emulator is trained on all but one of the model runs. In training our emulator, we chose to leave out ice sheet model run 67 from Applegate et al. (2012). This run 1) generates a zonal-mean ice thickness profile that is reasonably similar to observations, and 2) has parameter values that lie near the middle of the prior range, to avoid complications associated with extrapolation. We refer to the output (specifically, the zonal mean ice thickness profile and the ice volume change projection) from this left-out model run as our "assumed truth." Before using the mean ice thickness profile from our assumed-true model run in our perfect model experiment, we contaminate it with spatially-correlated errors (see the Supporting Information for details). These spatially-correlated errors reflect the discrepancies that we would expect to see between model output and data in a "real" calibration experiment, due to missing or parameterized processes in the model.

We first summarize each of the 100 model runs presented by Applegate et al. (2012) in terms of five input parameters and 10 principal component magnitudes, or 15 values in total. The ice sheet model can be thought of as a function that relates input parameter combinations to gridded, simulated modern ice thicknesses. We take the mean of each row in the grid, thereby obtaining a 264-element vector of zonally-averaged ice thicknesses for each ice sheet model run. We then apply principal component analysis to these mean ice thickness vectors. The magnitudes of the first 10 principal components

suffice to recover the mean ice thickness vectors.

Next, we train a Gaussian process emulator on all but one of the summarized ice sheet model runs. Because the principal components are independent by construction, each of their magnitudes can be related to the five input parameters by a separate instance of the emulator. The principal components and the emulator-estimated magnitudes can then be combined linearly to estimate the zonally-averaged ice thickness vector for any parameter combination, including those not already tested with the full ice sheet model.

We then use Markov chain Monte Carlo (MCMC) to estimate the joint posterior probability distribution over the five-dimensional input parameter space. MCMC is a well-established (Hastings, 1970), but complex, statistical technique; Brooks et al. (2011) provide a book-length treatment. Briefly, the Metropolis-Hastings algorithm used in MCMC constructs a sequence of parameter combinations, each of which is chosen randomly from the region of parameter space surrounding the last point. Candidate parameter combinations are accepted if the posterior probability of the new point is greater than at the previous one, or with a certain probability determined by the Metropolis-Hastings acceptance ratio otherwise. If the candidate point is rejected, another candidate point is chosen at random according to a proposal distribution. Consistent with McNeall et al. (2013), we match the emulator estimates to assumed-true model output instead of observed ice thickness values (Bamber et al. 2001, 2013) because we expect that the simplifications involved in constructing the ice sheet model (e.g., Kirchner et al. 2011) will cause problems in matching the modeled ice sheet to observed ice thicknesses. The candidate points that are retained by the MCMC algorithm approximate the posterior probability distribution of the input parameter space. The candidate points from this algorithm therefore reflect various characteristics of the posterior distribution, including the marginal distributions of each of the parameters separately and their joint distributions. Hence, we can use MCMC to summarize what we

have learned about the parameters from the model and observations while accounting for various uncertainties and prior information.

Finally, to achieve goal #3, we use a separate Gaussian process emulator to interpolate between the ice
280   volume change projections from all the model runs in the original ensemble (Applegate et al., 2012), except the assumed-true realization. When applied to the sample of the model input parameters that we obtained from Markov chain Monte Carlo, this emulator yields a sample of ice volume changes, and thus sea level rise contributions, between 2005 and 2100. We then used kernel density estimation to compute the probability density of the projected sea level rise contributions. It should be noted that
285   these projections are based on synthetic data (not real observations), and do not represent "real" projections of Greenland Ice Sheet mass loss over this century.

3. Results

290

Besides helping to diagnose interactions among ice sheet model parameters, our perfect model experiment allows us to test our overall procedure. We carry out several checks:

1) If the trained emulator is given the parameter settings from the left-out model realization, it should produce a close approximation to the actual output from that realization.

295   2) The maximum of the multidimensional posterior probability function from our Markov chain Monte Carlo analysis should lie close to the parameter settings from the left-out model realization.

3) The mode of the probability density function of ice loss projections should be close to the ice loss projection from the assumed-true model realization.

As detailed below, our methods pass all three of these checks.

300

Aggregating the ice thicknesses to their zonal means allows easy visual comparison of different emulator-estimated ice thickness vectors to the assumed-true model realization (black curve, Fig. 1). Parameter combinations yielding zonally-averaged ice thickness curves that lie close to the assumed-true model realization (e.g., the red curve in Fig. 1) are more likely (more probable based on the posterior distribution) than those with curves that lie farther from the assumed-true values (blue and green curves in Fig. 1).   Thus, our methods pass check #1, above.

The emulator, as trained on 99 of the model realizations from the Applegate et al. (2012) ensemble, successfully recovers the ice thicknesses from the left-out model realization (Fig. 2) when given the parameter combination for that left-out model realization as input.   Differences between the assumed-true and emulated zonally-averaged ice thickness vectors are minor.   Similarly, the conditional posterior density functions (Fig. 3) have maxima near the assumed-true parameter values.   We do not expect that the modes of the marginal posterior density functions (Fig. 4b) will fall exactly at the assumed-true parameter values, because summing over one or more dimensions often moves the marginal mode away from the maximum of the multidimensional probability density function.   In any case, the maximum posterior probability is close to the assumed-true parameter combination.   Thus, our methods pass check #2, above.   Some of the two-dimensional marginal probability density functions (Fig. 4b) show multiple modes and bands of high probability extending across the two-dimensional fields; we discuss the significance of these features below.

For comparison, we also produced scatterplots of parameter combinations as projected onto two-dimensional slices through the five-dimensional parameter space (Fig. 4a), following Applegate et al. (2012, their Fig. 1).   As in Applegate et al. (2012), the "successful" design points show no clustering around the assumed-true parameter values.

Our method also successfully recovers the ice volume loss produced by the assumed-true model realization (Fig. 5), reflected by the close correspondence between the mode of the probability density function produced by our methods and the vertical black line. Thus, our methods pass check #3, listed above. As previously noted, these projections are based on synthetic data; they are not "real" projections of Greenland Ice Sheet mass loss. For comparison, we also applied the windowing approach used by Applegate et al. (2012) to the model runs. The 95% probable interval produced by our methods is much smaller than that estimated by Applegate et al. (2012), reflecting the utility of spatial information in reducing projection uncertainties.

The prior density for the ice volume loss was constructed by assuming all 99 design points used to train our emulator are equally likely. Interestingly, a uniform prior for the input parameters results in a skewed and multimodal prior distribution for the volume loss, indicating that the function that maps input parameters to projected ice volume changes is highly non-linear and not smooth. These characteristics also cause a small offset between the assumed-true projection and the mode of the posterior density. The marginal plots for the volume loss projection surfaces are shown in Figure S1 in the supporting material.

4. Discussion

As explained above, our goals for this work were to identify an objective function for matching ice sheet models to spatially-distributed data (especially ice thicknesses), map interactions among model input parameters, and develop methods for projecting future ice sheet mass loss, with well-characterized uncertainties. We demonstrated that our emulator reproduces a vector of zonally-averaged ice thicknesses from a given model run when trained on other members from the same

14

ensemble (Fig. 2). We further showed that the emulator can recover the appropriate parameter combinations for an assumed-true model realization in a perfect model experiment (Figs. 3, 4b). Finally, we produced illustrative projections of Greenland Ice Sheet mass loss, based on synthetic data (Fig. 5). As noted above, our projections are for illustration only, and do not represent "real" projections of future Greenland Ice Sheet mass loss.

The utility of our approach becomes clear in comparing the marginal posterior probability density functions (Fig. 4a) and projections (red probability density function and boxplot in Fig. 5) to results from simpler methods (Fig. 4b; blue boxplot in Fig. 5; Applegate et al. 2012). In Figure 4b, there are distinct modes in the marginal densities, indicating regions of parameter space that are more consistent with the assumed truth. These modes are absent in the simpler graphic (Fig. 4b). Similarly, the 95% probable interval of sea level rise contributions is narrower using our methods than if a simple windowing approach is applied (Fig. 5).

The parameter interactions identified in this experiment are generally consistent with intuition (see Section 1.2.1 for descriptions of anticipated parameter interactions). Figure 4 shows inclined bands of high marginal posterior probability in the ice positive degree-day vs. snow positive degree-day, geothermal heat flux vs. ice flow factor, and basal sliding factor vs. flow factor panels. As expected, there are tradeoffs among each of these parameter pairs; for example, a low ice positive degree-day factor must be combined with a high snow positive degree-day factor to produce a reasonable match to the assumed truth. Somewhat surprisingly, the tradeoff between the geothermal heat flux and the ice flow factor is much stronger than that between the geothermal heat flux and the basal sliding factor. The geothermal heat flux affects both ice deformation (which is temperature-sensitive) and basal sliding (which operates only where there is liquid water at the ice-bed interface). We hypothesize that the geothermal heat flux has a stronger effect on ice flow than basal sliding because ice deformation

happens over a much larger fraction of the ice sheet's basal area than does sliding.

Multiple modes appear in the two-dimensional marginal density plots (Fig. 4), implying that standard methods for tuning of ice sheet models may converge to "incorrect" parameter combinations. Ice sheet models are commonly tuned by manually adjusting one parameter at a time until the simulated modern ice sheet resembles the real one (e.g., Greve et al. 2011). This procedure is an informal variant of so-called gradient descent methods, which search for optimal matches between models and data by moving down a continuous surface defined by the model's input parameters, the objective function, and the data. If the surface has multiple "peaks," gradient descent methods can converge to a point which produces a better match to the data than any adjacent point, but is nevertheless far from the "true" parameter combination. This problem may partly explain the wide variation in projections of sea level rise from the ice sheets, as made with state-of-the-art ice sheet models (cf. Bindschadler et al. 2013): even if the models had similar structures and reproduced the modern ice sheet equally well, we would still expect their future projections to diverge because of differences in input parameter choice.

4.1. Cautions and future directions

Our results are subject to several important limitations. First, we adjust only five model parameters. Our list of tested parameters is broadly consistent with other ice sheet model sensitivity studies (e.g., Ritz et al. 1997; Stone et al. 2010), but is still only a subset of the parameters that go into ice sheet models (e.g., Fitzgerald et al. 2011). In particular, we leave the exponent of Glen's flow law constant at 3, even though model-estimated ice velocities depend strongly on this deeply uncertain value (Cuffey and Kavanaugh 2011). Second, we match only a two-dimensional profile of zonally-averaged ice thicknesses from an assumed-true model run, rather than the two-dimensional grid of observed ice thicknesses (Bamber et al. 2001, 2013; see also McNeall et al. 2013). Finally, the simplifications built

into the ice sheet model that we use (SICOPOLIS; Greve 1997; Greve et al. 2011; see also Kirchner et al. 2011; van der Berg, 2011) inevitably cause differences between model output and the ice sheet's actual behavior. Correcting any of these issues would undoubtedly change our marginal posterior probability distributions (Fig. 3).

405

Our method can be expanded to treat the full, two-dimensional ice thickness grid and take advantage of other spatially-distributed data sets (e.g., surface velocities; Joughin et al. 2010). The long-term goal of this work is to compare ice sheet model runs to actual data, thereby resulting in probabilistic projections of future ice sheet mass loss.

410

5. Conclusions

In this paper, we presented an approach for probabilistic calibration of ice sheet models using spatially-
415   resolved ice thickness information. Specifically, we constructed a probability model for assigning posterior probabilities to individual ice sheet model runs, and used a Gaussian process emulator to interpolate between existing ice sheet model simulations. We reduced the dimensionality of the emulation problem by reducing profiles of mean ice thicknesses to their principal components. Finally, we showed how the posterior probabilities from the model calibration exercise can be used to
420   make projections of future sea level rise from the ice sheets.   In a perfect model experiment where the "true" parameter settings and future contributions of the ice sheet to sea level rise are known, our methods successfully recovered these values.   The posterior probability density function that resulted from this experiment shows tradeoffs among parameters and multiple modes.   The tradeoffs are consistent with physical expectations, whereas the multiple modes may indicate that commonly-applied
425   methods for tuning ice sheet models can lead to calibration errors.

Acknowledgements

440

Author contributions

WC designed the emulator, carried out the analyses, and wrote the first draft of the Supplementary Information. PJA wrote the first draft of the body text and supplied the previously-published ice sheet

445 model runs (available online at http://bolin.su.se/data/Applegate-2011). WC, PJA, MH, and KK jointly designed the research and edited the paper text.

References

450

Alley, R. B., Andrews, J. T., Brigham-Grette, J., Clarke, G. K. C., Cuffey, K. M., Fitzpatrick, J. J., Funder, S., Marshall, S. J., Miller, G. H., Mitrovica, J. X., Muhs, D. R., Otto-Bliesner, B. L., Polyak, L., and J. W. C. White, 2010: History of the Greenland Ice Sheet: paleoclimatic insights. Quat. Sci. Rev., 29, 1728-1756.

455

Applegate, P. J., Kirchner, N., Stone, E. J., Keller, K., and R. Greve, 2012: An assessment of key model parametric uncertainties in projections of Greenland Ice Sheet behavior. The Cryosphere, 6, 589-606.

Bamber, J. L., and W. P. Aspinall, 2013: An expert judgement assessment of future sea level rise from 460 the ice sheets. Nature Clim. Change, 3, 424-427.

Bamber, J. L., Layberry, R. L., and S. P. Gogineni, 2001: A new ice thickness and bed data set for the Greenland ice sheet 1. Measurement, data reduction, and errors. J. Geophys. Res., 106, 33,773-33,780.

465 Bamber, J. L., Griggs, J. A., Hurkmans, R. T. W. L., Dowdeswell, J. A., Gogineni, S. P., Howat, I., Mouginot, J., Paden, J., Palmer, S., Rignot, E., and D. Steinhage, 2013: A new bed elevation dataset for Greenland. The Cryosphere, 7, 499-510.

Bindschadler, R. A., Nowicki, S., Abe-Ouchi, A., Aschwanden, A., Choi, H., Fastook, J., Granzow, G., 470 Greve, R., Gutowski, G., Herzfeld, U., Jackson, C., Johnson, J., Khroulev, C., Levermann, A., Lipscomb, W. H., Martin, M. A., Morlighem, M, Parizek, B. R., Pollard, D., Price, S. F., Ren, D., Saito, F., Sato, T., Seddik, H., Seroussi, H., Takahashi, K., Walker, R., and W. L. Wang, 2013: Ice-sheet model

sensitivities to environmental forcing and their use in projecting future sea level (the SeaRise project). J. Glaciol., 59, 195-224.

475

Born, A., and K. H. Nisancioglu, 2012: Melting of northern Greenland during the last interglaciation. The Cryosphere, 6, 1239-1250.

Braithwaite, R. J., 1995: Positive degree-day factors for ablation on the Greenland ice sheet studied by

480   energy-balance modelling.   J. Glaciol., 41, 153-160.

Brooks, S., Gelman, A., Jones, G., and X.-L Meng, eds., 2011: Handbook of Markov chain Monte Carlo. Chapman and Hall/CRC, 619.

485   Calov, R., and R. Greve, 2005: A semi-analytical solution for the positive degree-day model with stochastic temperature variations.   J. Glaciol., 51, 173-175.

Chang, W., Haran, M., Olson, R., and K. Keller, 2013: Fast dimension-reduced climate model calibration.   arXiv preprint, arXiv:1303.1382.

490

Church, J. A., and N. J. White, 2006: A 20th century acceleration in global sea-level rise.   Geophys. Res. Lett., 33, L01602.

Cuffey, K. M., and J. L. Kavanaugh, 2011: How nonlinear is the creep deformation of polar ice?   A

495   new field assessment.   Geology, 39, 1027-1030.

Fitzgerald, P. W., Bamber, J. L., Ridley, J. K., and J. C. Rougier, 2012: Exploration of parametric

uncertainty in a surface mass balance model applied to the Greenland ice sheet. J. Geophys. Res., 117, F01021.

500

Fyke, J. G., Weaver, A. G., Pollard, D., Eby, M., Carter, L., and A. Mackintosh, 2011: A new coupled ice sheet/climate model: description and sensitivity to model physics under Eemian, Last Glacial Maximum, late Holocene and modern climate conditions. Geosci. Model Dev., 4, 117-136.

505   Greve, R., 1997: Application of a polythermal three-dimensional ice sheet model to the Greenland Ice Sheet: response to steady-state and transient climate scenarios. J. Clim., 10, 901-918.

Greve, R., and S. Otsu, 2007: The effect of the north-east ice stream on the Greenland Ice Sheet in changing climates. The Cryosphere Discuss., 1, 41-76.

510

Greve, R., Saito, F., and A. Abe-Ouchi, 2011: Initial results of the SeaRISE numerical experiments with the models SICOPOLIS and IcIES for the Greenland Ice Sheet. Ann. Glaciol., 52, 23-30.

Grinsted, A., Moore, J. C., and S. Jevrejeva, 2009: Reconstructing sea level from paleo and projected
515   temperatures, 200 to 2100 AD. Clim. Dyn. doi: 10.1007/s00382-008-0507-2.

Hastings, W. K., 1970: Monte Carlo sampling methods using Markov chains and their applications. Biometrika, 57, 97-109.

520   Hebeler, F., Purves, R. S., and S. S. R. Jamieson, 2008: The impact of parametric uncertainty and topographic error in ice-sheet modelling. J. Glaciol., 54, 899-919.

Heimbach, P., and V. Bugnion, 2009: Greenland ice-sheet volume sensitivity to basal, surface and initial conditions derived from an adjoint model. Ann. Glaciol., 50, 67-80.

525

Huybrechts, P., 2002: Sea-level changes at the LGM from ice-dynamic reconstructions of the Greenland and Antarctic ice sheets during the glacial period. Quat. Sci. Rev. 21, 203-231.

Jevrejeva, S., Moore, J. C., Grinsted, A., and P. L. Woodworth, 2008: Recent global sea level

530 acceleration started over 200 years ago? Geophys. Res. Lett 35, L08715.

Jevrejeva, S., Moore, J. C., and A. Grinsted, 2012: Sea level projections to AD2500 with a new generation of climate change scenarios. Glob. Planet. Change 80-81, 14-20.

535 Joughin, I., Smith, B. E., Howat, I. M., Scambos, T., and T. Moon, 2010: Greenland flow variability from ice-sheet-wide velocity mapping, J. Glaciol., 56, 415-430.

Kennedy, M. C., and A. O'Hagan, 2001: Bayesian calibration of computer models. J. R. Statist. Soc. B, 63, 425-464.

540

Kirchner, N., Hutter, K., Jakobsson, M., and R. Gyllencreutz, 2011: Capabilities and limitations of numerical ice sheet models: a discussion for Earth-scientists and modelers. Quat. Sci. Rev., 30, 3691-3704.

545 Lemke, P., Ren, J., Alley, R. B., Allison, I., Carrasco, J., Flato, G., Fujii, Y, Kaser, G., Mote, P., Thomas, R. H., and T. Zhang, 2007: Observations: changes in snow, ice, and frozen ground, in Solomon, S., Qin, D., Manning, M., Chen, Z., Marquis, M., and three others, eds., Cambridge University Press,

Cambridge.

550   Lempert, R., Sriver, R. L., and K. Keller, 2012: Characterizing uncertain sea level rise projections to support investment decisions. California Energy Commission Report CEC-500-2012-056.

Lenton, T. M., Held, H., Kriegler, E., Hall, J. W., Lucht, W., Rahmstorf, S., and H. J. Schnellnhuber, 2008: Tipping elements in the Earth's climate system. Proc. Natl. Sci. Acad. 105, 1786-1793.

555

McKay, M. D., Beckman, R. J., and W. J. Conover, 1979: A comparison of three methods for selecting values of input variables in the analysis of output from a computer code. Technometrics 21, 239–245.

McNeall, D. J., Challenor, P. G., Gattiker, J. R., and Stone, E. J., in review 2013: The potential of an

560   observational data set for calibration of a computationally expensive computer model. Geosci. Model Dev. Discuss., 6, 2369-2401.

Meehl, G. A., Stocker, T. F., Collins, W. D., and 11 others, 2007: Global climate projections, in Solomon, S., Qin, D., Manning, M., Chen, Z., Marquis, M., and three others, eds., Cambridge

565   University Press, Cambridge.

Pfeffer, W. T., Harper, J. T., and S. O'Neel, 2008: Kinematic constraints on glacier contributions to 21st-century sea-level rise. Nature, 321, 1340-1343.

570   Pollard, D., and R. M. DeConto, 2012: A simple inverse method for the distribution of basal sliding coefficients under ice sheets, applied to Antarctica. The Cryosphere, 6, 953-971.

Rahmstorf, S., 2007: A semi-empirical approach to projecting future sea-level rise. Science 315, 368-370.

575

Ritz, C., Fabre, A., and A. Letreguilly, 1997: Sensitivity of a Greenland Ice Sheet model to ice flow and ablation parameters: consequences for the evolution through the last climatic cycle. Clim. Dyn., 13, 11-24.

580   Robinson, A., Calov, R., and Ganopolski, A. 2010: An efficient regional energy-moisture balance model for simulation of the Greenland Ice Sheet response to climate change. The Cryosphere, 4, 129-144.

Rutt, I. C., Hagdorn, M., Hulton, N. R. J., and A. J. Payne, 2009: The Glimmer community ice-sheet
585   model. J. Geophys. Res.-Earth, 114, F02004.

Sacks, J., Welch, W. J., Mitchell, T. J., and H. P. Wynn, 1989: Design and analysis of computer experiments (with discussion). J. Statist. Sci., 4, 409-423.

590

Seddik, H., Greve, R., Zwinger, T., Gillet-Chaulet, F., and O. Gagliardini, 2012: Simulations of the Greenland ice sheet 100 years into the future with the full Stokes model Elmer/Ice. J. Glaciol., 58, 427-440.

595   Stone, E. J., Lunt, D. J., Rutt, I. C., and E. Hanna, 2010: Investigating the sensitivity of numerical model simulations of the modern state of the Greenland ice-sheet and its future response to climate change. The Cryosphere, 4, 397-417.

Urban, N. M., and T. E. Fricker, 2010: A comparison of Latin hypercube and grid ensemble designs for

600   the multivariate emulation of an Earth system model.   Computers and Geosciences, 36, 746-755.

van der Berg, W. J., van den Broeke, M., Ettema, J., van Meijgaard, E., and F. Kaspar, 2011: Significant

contribution of insolation to Eemian melting of the Greenland ice sheet. Nat. Geosci., 4, 679-683.

605   Vizcaino, M., Mikolajewicz, U., Jungclaus, J., and G. Schurgers, 2010: Climate modification by future

ice sheet changes and consequences for ice sheet mass balance.   Clim. Dyn., 34, 301-324.
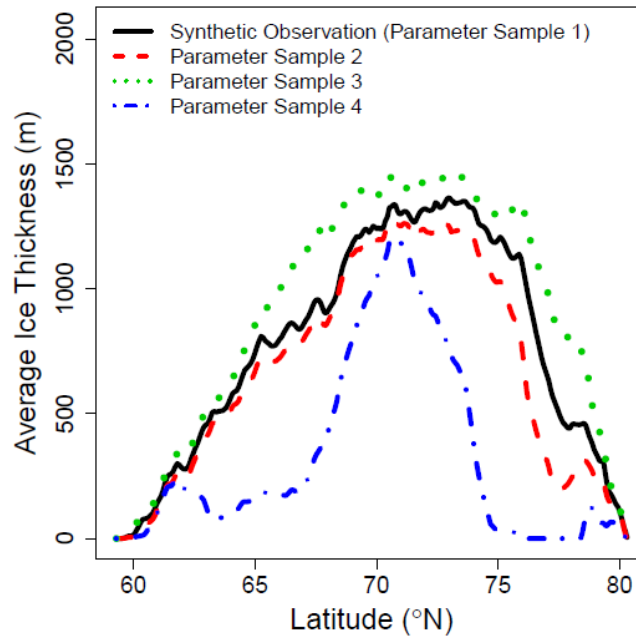
Figures

610

Figure 1. Profiles of zonal mean ice thicknesses from four different evaluations of the ice sheet model

SICOPOLIS (Greve, 1997; Greve et al., 2011). The solid black curve represents model run #67 from

Applegate et al. (2012), which we take to be the synthetic truth for our perfect model experiments.

615 The other curves represent examples of model runs used to construct the emulator: one run produces a

zonal mean ice thickness curve similar to the synthetic observations (dashed red curve), another is

generally too thick (dotted green curve), and a third is generally too thin (dotted and dashed blue curve).

As expected, our probability model assigns a greater posterior probability to the model run represented

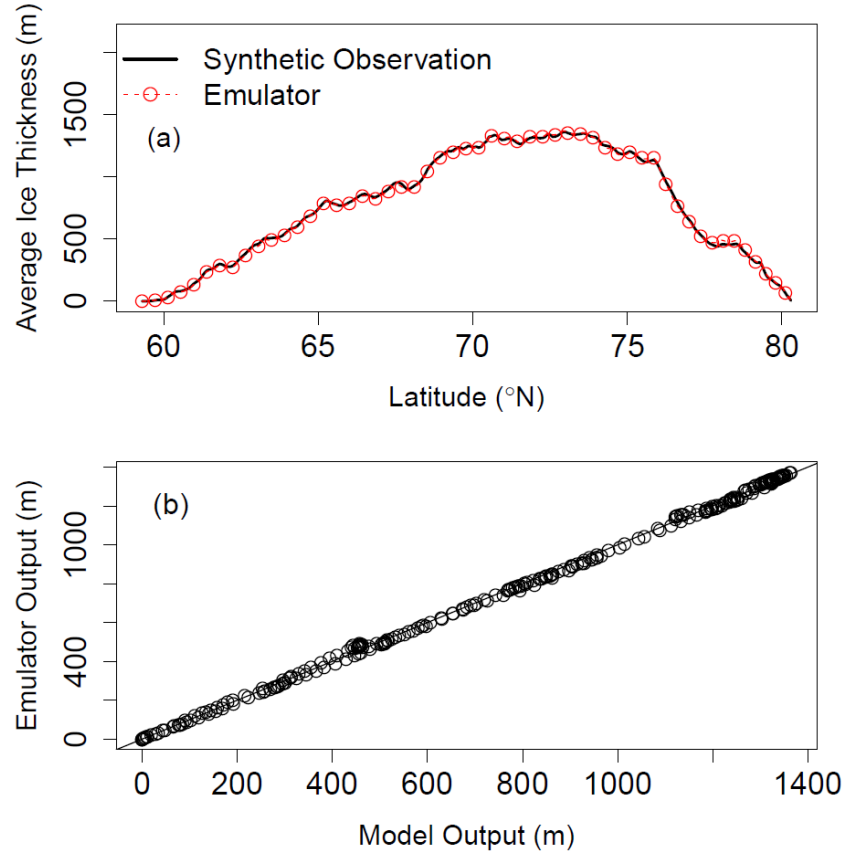by the red curve than to the model runs represented by the blue and green curves.

620

Figure 2. Comparison of zonal mean ice thickness transects from the assumed-true model run (#67 from Applegate et al., 2012) and that generated by the trained emulator at the same parameter combination as used in the assumed-true model run. In the top panel, the assumed-true profile is shown by a solid black line, and the emulator output is shown by a dashed red curve with circles. In the lower panel, each point stands for an individual latitude location. The red circles in the top panel fall almost exactly on top of the black curve, and the points in the lower panel fall almost exactly on a 1:1 line connecting the lower left and upper right corners of the plot. Thus, the emulator successfully recovers the ice thicknesses from an assumed-true model realization when trained on the other model runs from the same ensemble.
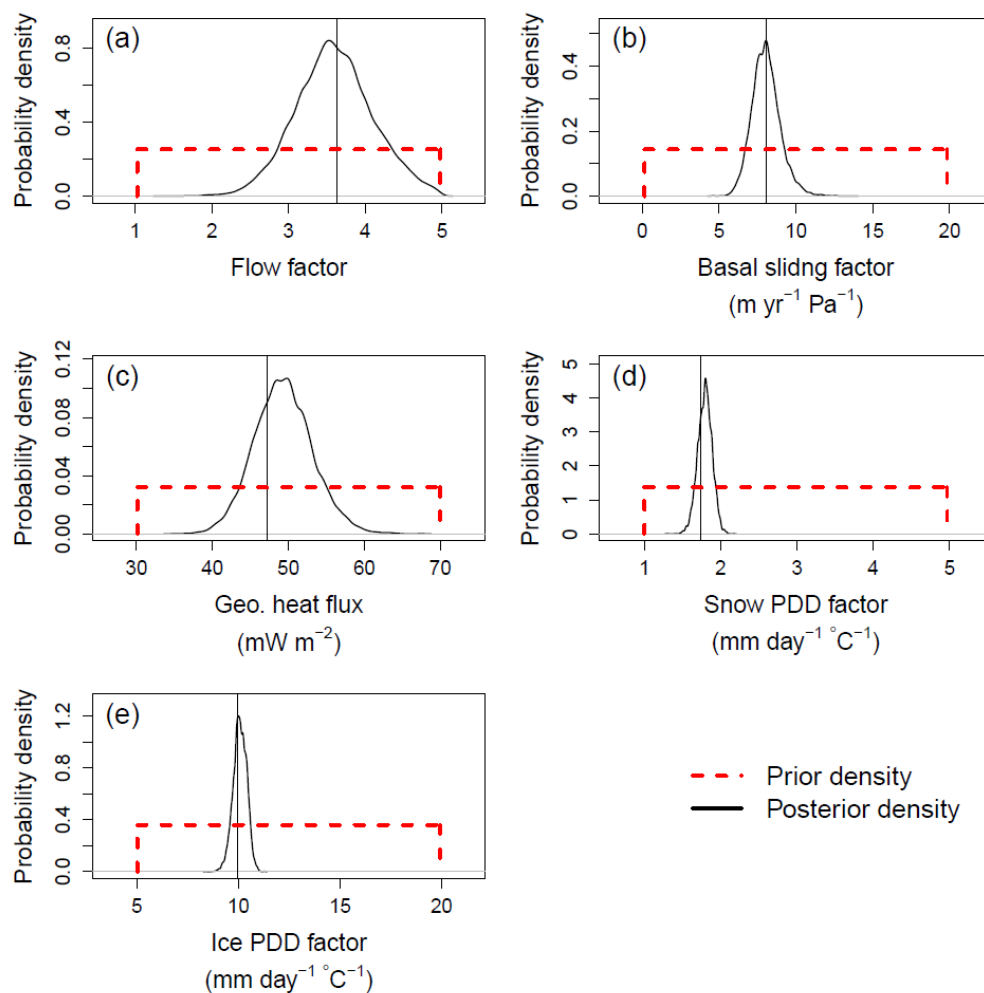
Figure 3. Prior (dashed red curves) and posterior (solid black curves) probability density functions of each input parameter, assuming that all the other parameters are held fixed at their assumed-true values. The vertical lines indicate the assumed-true values of the individual parameters.
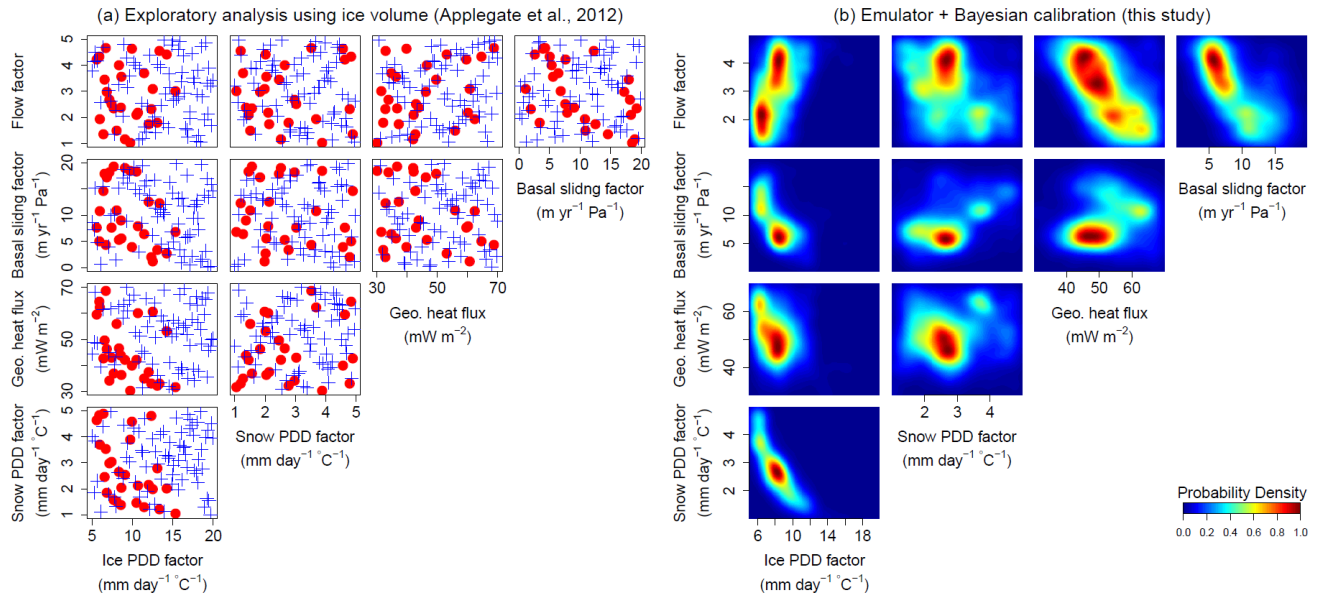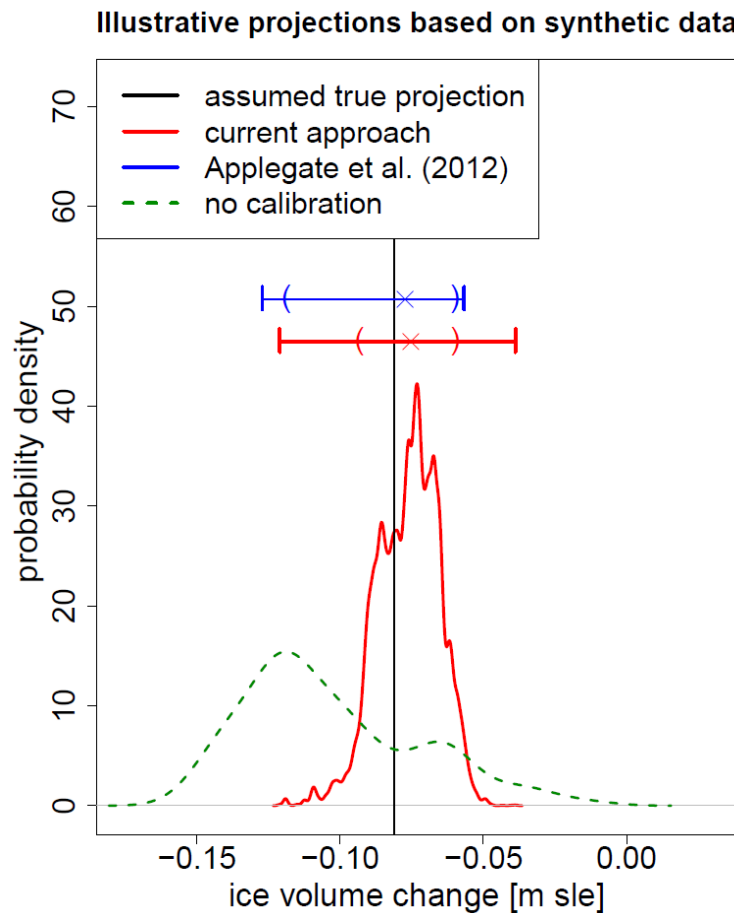
635

640

Figure 4. Comparison between an exploratory data analysis, following Applegate et al. (2012), and the results of our probabilistic calibration. (a) Scatterplots of parameter settings used to train the emulator, as projected onto two-dimensional marginal spaces. Red dots, parameter settings resulting in simulated modern ice volumes within 10% of the synthetic truth (model run #67 of Applegate et al. 2012); blue crosses, parameter settings that yield ice volumes more than 10% larger or smaller than the synthetic truth. (b) Two-dimensional marginal posterior densities of all pairs of input parameters. Several of the marginal posterior density maps show inclined bands of higher probability, indicating interactions among parameters; other panels show multiple modes, representing potential "traps" for tuning of ice sheet models using simpler methods. See text for discussion.

Illustrative projections based on synthetic data

655

Figure 5. Illustrative (not "real") ice volume change projections between 2005 and 2100, based on three different methods: i) the prior density of the input parameters (dashed green line); ii) parameter settings that pass the 10% ice volume filter used by Applegate et al. (2012) (solid blue line); and iii) the posterior density computed by our calibration approach (solid red line). The vertical line shows the ice

660 volume change projection for the assumed-true parameter setting. The horizontal lines and the parentheses on them represent the range and the 95% prediction intervals, respectively; the crosses indicate the median projection from each method. The width of the 95% projection interval from our methods is narrower than if simpler methods are applied (blue boxplot; Applegate et al., 2012). See text for discussion. m sle, meters of sea level equivalent.

665